Life-long Dietary Pesticides Cocktail Induces Astrogliosis Along with Behavioral Adaptations and Activates p450 Metabolic Pathways

Wendy Klement, Fabiana Oliviero, Giuseppe Gangarossa, Emma Zub, Frédéric de Bock, Isabel Forner-Piquer, Marine Blaquière, Frédéric Lasserre, Jean-Marc Pascussi, Tangui Tm Maurice, et al.

Life-long dietary pesticides cocktail induces astrogliosis along with behavioral adaptations and activates p450 metabolic pathways

Wendy Klement[1]*, Fabiana Oliviero[2]*, Giuseppe Gangarossa[3], Emma Zub[1], Frederic De Bock[1], Isabel Forner[1], Marine Blaquiere[1], Frederic Lasserre[2], Jean-Marc Pascussi[1], Tangui Maurice[4], Etienne Audinat[1], Sandrine Ellero-Simatos[2], Laurence Gamet-Payrastre[2], Laila Mselli-Lakhal[2] and Nicola Marchi[1]

[1]Institute of Functional Genomics (UMR 5203 CNRS – U 1191 INSERM, University of Montpellier), Montpellier, France.
[2]Toxalim (Research Centre in Food Toxicology), Université de Toulouse, INRAE, ENVT, INP-Purpan, UPS, 31300, Toulouse, France
[3]Université de Paris, BFA, UMR 8251, CNRS, F-75013 Paris, France
[4]MMDN, University of Montpellier, EPHE, INSERM, UMR_S1198, Montpellier, France

*Equal Contribution

Number of pages: 31
Words main text: 7,557
Figures: 8
Tables: 1
Supplemental Tables: 1

Running Title: Dietary environmental contaminants and brain-peripheral modifications

Keywords: pesticides cocktail, behavior, memory, electroencephalography, P450 enzymes, detoxification, metabolism, astrocytes

#Corresponding Author: Dr. Nicola Marchi, Cerebrovascular and Glia Research, Institut de Génomique Fonctionnelle (CNRS UMR5203, INSERM U1191, University of Montpellier), 141 rue de la Cardonille, 34094 Montpellier, Cedex 5, France. Email nicola.marchi@igf.cnrs.fr.

Acknowledgements. This work was support by ANR-Hepatobrain, ANSES Epidemicmac, MUSE-iSite University of Montpellier.

Abstract

Exposure to environmental contaminants is a public health concern. However, pre-clinical studies examining the impact of pesticides at low-dose and their long-term consequences are uncommon. Here, C57BL6/j male and female mice were daily fed from weaning and up to 12 months, corresponding to early-childhood into middle-age in humans, using chow pellets containing a cocktail of pesticides and exposing them to the tolerable daily intake level for each pesticide. We found that 12 months of dietary exposure to pesticides was associated with a moderate astrogliosis in the hippocampus. The expression of platelet-derived growth factor receptor beta (PDGFRβ), an indicator of pro-fibrotic tissue changes, was modified at the perivascular level. Examination of Iba1^{+} microglial cells did not reveal sizeable changes. Concomitantly to astrogliosis, spontaneous spatial memory and sociability were impaired in males at 12 months of dietary exposure to pesticides. Telemetry electrocorticograhic explorations ruled out the presence of epileptiform activity or theta-gamma wave modifications in these conditions. Long-term pesticides impacted the periphery where the hepatic P450 metabolic cytochromes Cyp4a14 and Cyp4a10 were significantly upregulated in male and female mice during the 12 months of exposure. The expression of β-oxidation genes, such as Acox1, Cpt1a and Eci, was also significantly increased in male and female mice in response to pesticides. Collectively, our results indicate that long-term exposure to pesticides cocktail elicits spatio-temporally restricted brain modifications and significant activation of P450 pathways in the periphery. These brain-peripheral adjustments are discussed as time-dependent vulnerability elements.

Highlights

1) Long-term pesticides exposure promotes a discrete astrogliosis in the hippocampus.

2) Long-term pesticide exposure is associated with sex-dependent spatial memory and sociability adaptations.

3) The continuous exposure to pesticides cocktail significantly activates peripheral P450 metabolic and β-oxidation enzymes.

Introduction

Epidemiological studies indicate environmental contaminant exposure as a significant risk factor for the development of central nervous system (CNS) and peripheral metabolic disorders (Hernandez et al., 2016, Kamel and Hoppin, 2004). Because of the widespread use and the omnipresence of pesticides cocktail in agricultural crops, which lead to an involuntary and continuous consumption, the relevance to public health is high. However, these accumulating epidemiological alarms are not properly harmonized with experimental studies examining the impact of pesticides using long-term protocols, cocktails, and dose ranges relevant to exposure in humans. In rodents, the effects of pesticides have been examined by using high doses of single molecules, often organophosphates, mimicking intoxication scenarios and not (sub)threshold chronic exposure (Banks and Lein, 2012, Czajka et al., 2019, Lushchak et al., 2018, Ojo et al., 2014, Pu et al., 2020). Under these conditions, neuroinflammation and cognitive impairments were reported (Banks and Lein, 2012). However, current studies do not address the critical question of whether a long-term dietary exposure to a low dose pesticides cocktail may be sufficient to promote similar pathological deviations.

Attention is also directed to the link between long-term exposure to pesticides and peripheral P450 detoxification or metabolic pathways. The rationale stems from accumulating evidence indicating a pathological interplay between peripheral metabolic diseases and neurological functions (Bogush et al., 2017, Donovan et al., 1998, Guillemot-Legris and Muccioli, 2017, Miller and Spencer, 2014, Rom et al., 2019, Sureka et al., 2015). Previous results published by our consortium indicated

that a long-term exposure to a pesticides cocktail, identical to the one used here, promotes obesogenic and diabetogenic effects (Lukowicz et al., 2018). Others have shown that a single high dose of pesticides can induce the expression of cytochromes (Cyp) enzymes (Abass et al., 2012). However, the possibility that a chronic exposure to a cocktail of pesticides at low doses may trigger modifications of P450 detoxification and metabolic pathways *in vivo* remains to be confirmed.

Here, we tracked and quantified a set of *in vivo* brain readouts and analyzed peripheral metabolic and detoxification pathways during a long-term exposure to dietary pesticides. To achieved this goal, we developed a protocol where C57BL6/j male and female mice were fed, starting from weaning (PN21) and for a long-term period of 12 months, with chow pellets containing a specific cocktail of pesticides that could be applicable to agriculture, as indicated by the European Food Safety Authority (EFSA) reports (Lukowicz et al., 2018). Six pesticides were incorporated in food pellets, exposing mice to the tolerable daily intake for each pesticide.

Methods

Vertebrate Animals

Research was conducted in accordance to the institutional guidelines for laboratory animal usage (European Union Council September 22, 2010 (2010/63). Protocols were approved by the French ethical committee (Apafis#13145-2018012216217153 v3). C57BL/6j male and female mice were housed (food and water *ad libitum*) in a 12h light/dark cycle, minimizing animal discomfort. The specific number of mice used for each experiment is detailed in the sections below and in the Figure legends.

Pesticides chow preparation

Male and female C57BL/6j mice were fed starting from weaning (PN21) using standard (control) or pesticides chow. The selected cocktail contains fungicides and insecticides (ziram, thiophanate, captan, chlorpyrifos, boscalid, and thiachlopride). The chow is routinely prepared by our research consortium, as previously reported (Lukowicz et al., 2018). In this study, mice were exposed to the tolerable daily intake (TDI; mg/kg body weight / day; see Table 1, readapted from (Lukowicz et al., 2018) for each pesticide. TDI is defined for humans by the EFSA and by the Joint Food and Agriculture Organization (United Nations, World Health Organization). TDI levels defined for human exposure were adjusted to mice body weight (BW). In our study, we considered a mouse BW of 30 grams and a daily chow intake of 5 grams. Table 1 specifies the quantities for each pesticide incorporated in the diet. Chow preparation:

pesticides were dissolved individually in a 9:1 volume / volume methanol:acetone and mixed together. The solution was dispersed on Vitaminic powder mixture-200 (Scientific Animal Food Engineering) and homogenized using a Rotavapor (Laborota 4000™; BUCHI Switzerland) for 30 minutes at 45°C and then at room temperature for 50 minutes to evaporate the solvents. The resulting powder was incorporated into the pellet (SAAJ-RAF National Research Institute for Agriculture, Food and the Environment, INRAE). Control diet was concomitantly prepared without adding pesticides. Pesticide levels in the pellet were re-analyzed by gas chromatography–tandem mass spectrometry and liquid chromatography–tandem mass spectrometry (Eurofins), confirming concentrations (Table 1; see also (Lukowicz et al., 2018)).

Brain immunohistochemistry and quantifications

Analyses were performed by using: i) n=8 pesticide diet and n=8 standard diet male mice at 3 months; ii) n=7 pesticide diet and n=8 standard diet female mice at 3 months; iii) n=8 pesticide diet and n=8 standard diet male mice at 12 months; iv) n=8 pesticide diet and n=8 standard diet female mice at 12 months (Figures 1 and 2). After intracardial perfusion with PBS, mice brains were dissected and fixed in PFA 4% solution. Fixed brains were immerged in sucrose 15% for 24h followed by sucrose 30%. Brains were then snap frozen and stored at -80°C. Slices (20-25µm) were obtained using a cryostat. Immunohistochemistry was performed after PBS washes. Slices were added with blocking solution (PBS, triton 0.5%, horse serum 20%) at room temperature for 1h. Primary antibodies (See Supplemental Table 1) were diluted in blocking solution and brain slices incubated overnight at 4°C. After

PBS washes, secondary antibody was added in PBS for 2h at room temperature. After PBS washes, slices were mounted using Vectashield containing DAPI.

For all quantifications, 20X Z-stack images (Z=12 to 15 planes, each of 1um) were analyzed using Fiji. Slices were examined for each mouse to quantify signals in the regions of interest (ROI) hippocampal CA1/CA2, CA3/DG, and neocortex (CTX), identified by DAPI maps. Prior to analysis, all Z-stacks images were combined (Z-project, sum) using Fiji. *GFAP quantification*: images were converted into RGB stack format and signal threshold was adjusted at around 200 units for each image. Area of GFAP signal was calculated setting a threshold sensitivity equal for each image. GFAP data are expressed as percentage of ROI total pixels. *Iba1 quantification*: a cell counter tool was used to calculate the total number of DAPI cells and the number of $Iba1^+$ cells in each ROI. Data are expressed as percentage ($Iba1^+$/tot $DAPI^+$) x 100. *CD13 pericyte quantification*: a skeleton plug-in was used to track CD13 signals and drawn vessels. The analysis was automated by setting threshold sensitivity identical for each image. Length was calculated as pixels. *PDGFRβ quantification*: signals were quantified using a Fiji freehand line tool to select signals associated and proximal to the $IsoB4^+$ vessels. The ROI Fiji manager was used to collect the dataset. Total vascular IsoB4 length was calculated using the skeleton Fiji tools for each image and used as reference.

Behavioral testing

We performed 2 sessions of behavioral tests (3 and 12 months of age). We analyzed: n=10 pesticide diet male, n=9 standard diet male, n=9 pesticide diet

female, n=10 standard diet female mice at 3 and 12 months (Figures 3 and 4). *Open field (OF)*. Spontaneous exploratory behavior was monitored in an OF (opaque black plastic arena, 35cm width x 50cm length x 20cm height) for 10min. The center zone was defined as a virtual perimeter within 5cm from the sides of the arena. Experiments were videotaped and an observer scored the time spent in the center and the number of transitions in the center zone. The arena was cleaned with 70% ethanol after each experiment. *Spatial working memory, spontaneous alternation in the Y-maze*. Each mouse was placed at the end of one arm in a grey polyvinylchloride Y-maze and allowed to freely explore during a single session (8 minutes). Arm entries, including possible returns into the same arm, were recorded visually. Alternation was defined as alternated entries into the three arms during consecutive trials. The percentage (%) of alternation was calculated as actual alternations/maximum alternations x 100. Measured parameters included the percentage of alternation (working memory index) and total number of arm entries (exploration index). All arms were cleaned with 70% ethanol between two sessions. *Light/Dark Transition test*. The apparatus consists of a cage (21x42x25cm) divided into two chambers, dark and bright, of equal size by a partition with door. Mice were allowed to move freely between the two chambers during 10min. The number of entries into the bright chamber and the duration of time spent there were measured by videotracking (Viewpoint, Lissieu, France). After each trial, all chambers were cleaned with 70% ethanol. *Elevated-Plus-Maze (EPM)*. The EPM is a 4-arms maze elevated 40cm above the floor. The 4 arms intersect to form a plus sign (dimension of each arm: length 30cm, width 5cm, and center region 5x5 cm^2). Two of the arms are closed on 3 sides by 15 cm high walls, and the other two are open. Animals were placed in the center of the apparatus and allowed to freely explore the maze for

10min. Score for entries and time spent in open arms were measured. All arms were cleaned with 70% ethanol after each experiment. *Social Interaction*. The apparatus is a rectangular 3-chambered polycarbonate box divided in three chambers. The test mouse was placed into the middle chamber and allowed to explore freely for 10min. The test was video-tracked (Viewpoint). Time spent in each chamber was analyzed to measure the side preference bias. Each of the 2 sides contained an inverted empty wire cup. After the habituation period, the test mouse was retired, an unfamiliar mouse was introduced into one of the empty wire cups. The test mouse was reintroduced and the time spent sniffing each wire cup was analyzed for 10min.

Freely moving, telemetry Video-electrocorticography monitoring

A total of 16 male and 16 female C57Bl/6 mice were monitored at 3 and 12 months (n=4/group, pesticides and control) by using telemetry. Because of technical issues (defective implants) 2 mice were excluded from the analysis. Surgical procedure: animals were anesthetized using i.p. chloral hydrate and xylazine (400mg/kg; 4mg/kg). Animals were placed on a heating pad during the procedure ensuring a physiological temperature. A telemetry implant (Physiotel transmitter ETA-F10, weight 1.6 g, 1.1 cm^3, Data Science international DSI, St Paul, MN, USA) was placed into a ventral pocket. The subcutaneous tissue covering the skull was separated and the periosteum cleaned. Two screws (one bipolar electrode) are inserted in the skull corresponding to the fronto-parietal neocortex. Screws were attached to the transmitter wires. Dental cement was used to fix the two screws to the skull. The incision was closed using a non-reabsorbable 6/0 suture material (prolene polyprolene, Ethicon) and stitches. Mice were allowed to recover for 1 week. Mice

were recorded (Dataquest ART software DSI) for at least 24 hours each, equally distributed between day and night. Signals were acquired at 500 Hz and analyzed using Neuroscore. Video analysis was executed by an operator to rule out motion artifacts (e.g., eating, drinking or chewing). Trace portions (1-5 minutes/extract, for a total of 30 minutes/mouse) were chosen considering light vs. dark phases, awake/exploratory vs. sleep/immobility, and avoiding all motion artifacts. Periodogram Power Bands (Neuroscore) was calculated for all EEG and the relative abundance of each 0.5 Hz increment (0.5–80 Hz) was quantified (Boussadia et al., 2016, Boussadia et al., 2018, Ichkova et al., 2020).

qPCR studies

We analysed a total of n=6 and n=8 mice of both sexes at 3 and 12 months (Figures 6, 7 and 8). Liver total RNA was extracted with TRIzol® reagent (Sigma-Aldrich). For real-time quantitative polymerase chain reaction (qPCR), total RNA samples (2 µg) were reverse-transcribed using a High Capacity cDNA Reverse Transcription Kit (Applied Biosystems, Courtaboeuf, France). Primers for SYBR Green assays are presented in Supplemental Table 1. Amplifications were performed on an ABI Prism 7300 Real Time PCR System (Applied Biosystems). qPCR data were normalized by TATA-box binding protein mRNA levels and analysed with LinRegPCR (2015.3 version). Identical protocol was used for kidney tissue.

Statistics

All data were analyzed using Prism 8.3.1. Dataset were not normally distributed (Shapiro-Wilk test) or did not present equal variance (Brown-Forsythe test) therefore a non-parametric ANOVA Kruskal-Willis followed by Dunn's multiple comparisons test was used for analysis of male and female groups. Results are reported as box and whiskers plots with single points and indicating median, interquartile ranges and min-max range. Significance threshold was set at $p < 0.05$.

Results

Impact of long-term pesticides cocktail exposure on brain cells

We examined the effects of long-term dietary pesticides on histological biomarkers of neuroinflammation, specifically glial fibrillary actin protein (GFAP), platelet derived growth factor receptor beta (PDGFRβ) expression, microglial Iba1, and CD13 pericytes. In male mice, astrogliosis occurred in the CA1/CA2 hippocampal regions following 12 months of exposure to dietary pesticides, as compared to other groups (Figure 1B1). Increased GFAP expression occurred at the parenchyma and perivascular levels (Figure 1A1-A2). In female mice, a trend in GFAP increase was observed after 12 months of pesticides exposure in the CA1/CA2 region as compared to sex and age matched control (Kruskal-Wallis and Dunn multiple comparisons test, p= 0.14; Figure 1B2). Female mice displayed a significant effect of aging, impacting GFAP reactivity in the hippocampus (Figure 1B2 and C2). GFAP reactivity was variable in females as compared to males, as assessed long-term in the CA hippocampal regions (Figure 1B1, B2 and C1, C2). In the neocortex, no significant GFAP astrogliosis was observed following pesticide-exposure, except for an increase at 3 months in male mice (Figure 1D1).

PDGFRβ reactivity, a sign of pro-fibrotic tissue modifications (Giannoni et al., 2020, Klement et al., 2019, Kyyriainen et al., 2017, Riew et al., 2018), was significantly increased specifically in the CA1/CA2 hippocampal regions of male mice at 12 months during pesticide exposure (Figure 2C1). Qualitatively, the increased of PDGFRβ signal occurred around the IsoB4^{+} capillaries and in the parenchyma where

PDGFRβ$^+$ cells were visible (Figure 2A1-A2). Female mice presented a significant increase in PDGFRβ$^+$ cells at 3 months during pesticides exposure (Figure 2C2). In the CA3/DG regions, the pesticides-induced PDGFRβ reactivity was more pronounced in female as compared to male mice, with no effect of aging (Figure 2D1-D2). A similar pattern was observed (Figure 2B1-B4) and quantified (Figure 2E1-E2) in the neocortex. In these experimental conditions, the percentage of hippocampal Iba1$^+$ microglial cells remained at a control level of ~10% (Li and Barres, 2018), except for a transient and minor increase in the CA3/DG region at 3 months during pesticides exposure (Kruskal-Wallis and Dunn multiple comparisons test, $p = 0.015$). As a corollary, we observed a lower number of microglial cells in female as compared to male mice at 12 months independently from pesticide exposure (*data not shown*). Finally, the number and the length of CD13$^+$ pericytes were generally unmodified by pesticides exposure, except for a localized increase of pericytes number in the CA1/CA2 hippocampal region in female mice at 12 months (Kruskal-Wallis and Dunn multiple comparisons test, $p = 0.037$). Age dependent effects were observed for female mice in the hippocampus (*data not shown*). Finally, qPCR analysis of pro-inflammatory cytokines, chemokines, or adhesion molecules (TNFa, CCL2, CCL12, CXCL5, ICAM1, VCAM) did not reveal significant changes across groups (*data not shown*). These results outline discrete and regional hippocampal cellular modifications, e.g., astrogliosis, following chronic dietary exposure to pesticides. Our results reveal the effect of aging on GFAP hippocampal reactivity.

Behavior analyses during long-term exposure to pesticides.

A battery of behavioral assessments was performed by tracking and re-testing each cohort of male and female (Figure 3 and 4 respectively) mice at 3 and 12 months during dietary exposure to pesticides. Body weight variations are indicated in Figure 3A and 4A. Because cellular modifications were studied in the hippocampus, here we tested the spatial working memory. A significant impairment in the spontaneous alternation behavior was observed for male mice exposed to pesticides during 12 months as compared to 3 months control mice (Figure 3B). This deficit was not accompanied by an altered number of entries in the Y-maze arms (Figure 3C). No differences in spatial working memory (Y-maze) were detected in females (Figure 4B-C). Male mice exposed to long-term (12 months) dietary pesticides also showed a significant reduction in social interaction time as assessed in the three-chambers test as compared to the 3 months group (Figure 3D). Using the open field (OF) test we observed a reduction in the spontaneous locomotor activity during the entire study which may indicate aging-dependent, but likely pesticides-independent, impairments (Figure 3E). The reduced locomotor drive was accompanied by an increase of time spent in the center zone of the OF in mice exposed to long-term dietary pesticides, suggesting a reduced anxiety behavior (Figure 3F). However, when tested in purely anxiety-related paradigms (light/dark box and EPM), pesticides-exposed male mice did not shown modifications as compared to control mice (Figure 3G, H). In female mice, except for a small and transient increase in the time spent in the center zone of the OF at 3 months during pesticides exposure (Figure 4F), no major anxiety-related deficits were observed (Figure 4B-H). Altogether, these results indicate that long-term

dietary pesticides impact on specific, but not generalized, behavioral outputs particularly in male mice.

Neurophysiological explorations during long-term exposure to pesticides.

Using a dedicated cohort of mice, we monitored the electro-corticographic activity at 3 and 12 months during pesticides exposure. The analysis of all traces ruled out the presence of repetitive spike activity, seizures or pro-epileptiform modifications in our experimental conditions (Figure 5A1-A4). We next examined the patterns of theta and gamma brain waves distribution, as indicators of neurological dysfunction (Iaccarino et al., 2018, Ichkova et al., 2020, Kitchigina, 2018, Mably and Colgin, 2018) during sleep/immobility and awake/exploration periods. Figure 5B1-B4 provides the entire spectrograms (0.5 to 80Hz) calculated for each mouse monitored. Pesticides exposure did not result in significant corticographic modifications as compared to sham, except for a transient segregation of theta (4-7Hz) and gamma (40-50Hz) frequencies occurring at 3 months between sham and pesticides exposed female mice during awake periods (Figure 5C3). These results indicate that, in these experimental conditions, long-term exposure to dietary pesticides does not associate with electrographic modifications that can be detected at the cortical level in vivo.

Activation of peripheral P450 metabolic and detoxification pathways during exposure to pesticides

The dietary exposure to the pesticides cocktail used here was previously shown to induce diabetogenic effects in vivo (Lukowicz et al., 2018). Consistent with

this existing research, we examined the effects of chronic pesticides exposure on the regulation of metabolic and detoxification pathways. To this end, the expression levels of target genes of the peroxisome proliferator-activated receptor alpha (PPARα), constitutive androstane and pregnane xenobiotic receptors (CAR, PXR) were quantified in the liver. The mRNA levels of the PPARα target genes Cyp4a14 and Cyp4a10 were increased in both male and female mice exposed to pesticides during 12 months (Figure 6A1-A4), with a trend increase already occurring at 3 months. Levels of CAR controlled Cyp2b10 and Cyp2C29 were unmodified except for an increase of Cyp2b10 specifically in male mice at 3 months (Figure 6B1-B4). The PXR controlled Cyp2c55 and Cyp3a11 enzymes were increased during pesticides exposure at 12 months, both in male and female mice and as compared to 3 months, indicating a predominant effect of aging (Figure 6C1-C4). Cyp2c55 was increased at 12 months in the pesticides exposed group. As a corollary, the patterns of Cyp expression were analyzed in kidney samples available from pesticides exposed animals at 12 months. Cyp4a14 and Cyp4a10 levels were increased over time in this organ in male and female mice in response to pesticides exposure (Figure 8A1-A2).

At the metabolic level and consistent with PPARα activation, the genes involved in ß-oxidation (Acox1, Cpt1α and Eci) and hepatic lipid transport (Cd36) were up-regulated following 12 months of pesticide exposure in males and females as compared to age and sex matched controls (Figure 7A1-A6 and B1, B3). Gene expression of Glut2, involved in glucose transport, was not modified by pesticides exposure (Figure 7B2, B4). Collectively, these results indicate that a life-long exposure to dietary pesticides induces a significant activation of specific nuclear receptors and enzymes involved in detoxification processes and in lipid metabolism.

Discussion

In this study, we report spatio-temporally confined hippocampal astrogliosis and perivascular pro-fibrotic modifications along with specific sex-dependent behavioral modifications elicited after long-term, but not short-term, dietary exposure to pesticides at low dose. Simultaneously, significant modifications of peripheral P450 metabolic and detoxification pathways were triggered and endured during pesticides exposure. If the direct association between the reported brain and peripheral changes remains to be fully examined, our results, together with our previously published data (Lukowicz et al., 2018), suggest that the outcome of a life-long exposure to low dose pesticides may be a vulnerability condition. The latter could be relevant to second pathological insult or further stress settings, supporting the significance of a 2-hits hypothesis. By study design, mice ingested the pesticides cocktail at every meal and during a significant portion of their lifespan, whereas human consumers may not experience such frequent intake and they may not be daily exposed to TDI levels.

Long-term pesticides exposure, astrogliosis and behavior: is there a potential association?

We report discrete and time-dependent astrogliosis along with specific behavioral alterations during long-term dietary pesticides exposure in male mice. Because microglia and pro-inflammatory cytokines expression were not significantly modified, the reported astrogliosis may also suggest metabolic cellular dysfunctions. Thus, by performing glycogenesis and lipid metabolism, astrocytes are important for

nutrients support of neurons, thus ensuring proper synaptic transmission (Deitmer et al., 2019, Morita et al., 2019). We also report sex-specific patterns of astrogliosis in response to pesticides exposure. Importantly, differences in astrocytes' number, activation patterns (Morrison and Filosa, 2016, Tassoni et al., 2019) and bioenergetic functions (Jaber et al., 2018) are sex-dependent and were previously reported in physiological (Mouton et al., 2002) and disease conditions (Santos-Galindo et al., 2011).

In general, astrocytes contribute to neurophysiology and maladaptive alterations of the astrocyte-neuron coupling that are critical for cognitive functions (Dallerac and Rouach, 2016, Pekny et al., 2016, Suzuki et al., 2011). The behavioral impairments here reported were not associated with other major deficits, thus suggesting that long-term exposure to dietary pesticides may represent a permissive, but not entirely sufficient, risk factor for long-lasting cognitive changes. Female mice presented no behavioral changes, supporting sex-specificity for the pesticide effects. We recognized that we did not control for estrus cycle, an important caveat as estradiol levels were shown to impact behavior (Azcoitia et al., 2010). We here discuss that the in vivo electrophysiological explorations did not reveal significant changes when comparing pesticides exposed to control animals. More sensitive monitoring tools are available to study single unit neuronal activity in vivo and in vitro and they should be used for next explorations in these experimental settings.

Experimental evidence has shown that intoxication by single pesticides (e.g., organophosphates) elicits an acute inflammatory response (Banks and Lein, 2012, Gangemi et al., 2016). Here, we report astrogliosis and pro-fibrotic modifications

occurring in a spatio-temporal manner during long-term pesticides exposure. However, our GFAP analysis did not allow distinguishing between astrocytes accumulation and altered morphology. Our results may fit within the proposed link between hippocampal inflammation and memory or sociability negative outcomes (Li et al., 2017, Pekny et al., 2016, Sofroniew, 2014, Stevenson and Caldwell, 2014). Interestingly, exposure to the herbicide glyphosate during pre- and post-natal stages was previously reported to elicit hippocampal GFAP reactivity and cognitive impairments (Ait-Bali et al., 2020). A link between glyphosate exposure, modification of brain soluble epoxide hydrolases expression, inflammation, and autism spectrum disorder was also proposed (Pu et al., 2020). Furthermore, available evidence showed an increase of hippocampal GFAP expression in mice exposed to chlorpyrifos or to malathion (dos Santos et al., 2016, Lim et al., 2011). Cell cultures from fetal rat telencephalon exposed to high levels of parathion and chlorpyirifos displayed increased GFAP immunostaining (Zurich et al., 2004). Dissecting the individual effects for each pesticide present in our cocktail is important and it should be studied in male and female mice. The notion of a cocktail effect was previously investigated for chlorpyrifos and abamectin, examining neurotoxicity following 30 days of exposure (Nasr et al., 2016). The combination of chlorphyrifos, permethrin and pyridostigmine bromide elicited significant GFAP reactivity, as compared to each compound tested individually (Ojo et al., 2014).

Peripheral-brain pathology during chronic pesticides exposure: initial clues

Epidemiological evidence links dietary pesticides to the increased risk for peripheral pathological modifications, including diabetes, obesity or insulin resistance

(Al-Eryani et al., 2015, Casals-Casas and Desvergne, 2011, Evangelou et al., 2016), with a possible extension to brain diseases (Gangemi et al., 2016, Hernandez et al., 2016, Kamel and Hoppin, 2004). Importantly, diabetes mellitus is associated with neurological disorders and signs of neuro-inflammation (Bogush et al., 2017, Donovan et al., 1998, Rom et al., 2019, Sureka et al., 2015). Obesity represents a risk factor for cognitive defects (Guillemot-Legris and Muccioli, 2017, Miller and Spencer, 2014). However, most epidemiological and experimental studies have focused on organochlorine pesticides (De Long and Holloway, 2017, Evangelou et al., 2016, Wang et al., 2014) and data relative to the impact of other pesticides are incomplete. Our results show a significant upregulation of peripheral P450 detoxification and metabolic pathways, while the obesogenic and diabetonegic effects of chronic exposure to low dose pesticides were previously reported by our research consortium (Lukowicz et al., 2018). Chronic exposure to pesticides resulted in the upregulation of genes controlled by the nuclear receptor PPARα, such as the detoxifying enzymes Cyp4a14 and Cyp4a10 in liver and kidneys, and β-oxidation genes. The augmented expression of metabolic enzymes can be either protective, by detoxifying pesticides or other toxins, or pathological by dysregulating the metabolism of endogenous steroids, hormones and xenobiotics, possibly leading to unpredictable drug kinetics or side-effects. The activation of the PPARα nuclear receptor in the liver can be beneficial (Nisbett and Pinna, 2018) and detrimental, and its chronic stimulation and the consequent upregulation of P450 genes may have contributed to the phenotype previously observed (Lukowicz et al., 2018). Furthermore, the possibility that pesticides exposure, as single or cocktail, could modify the expression of metabolic enzymes in the brain remains to be tested. Brain P450 enzymes were proposed to play a role in the metabolism of neurotransmitters and neurosteroids in

health and disease conditions, including alcohol intoxication, inflammation, and epilepsy (Ferguson and Tyndale, 2011, Ghosh et al., 2011, Runtz et al., 2018).

Conclusions

We provide the initial indication that dietary pesticides cocktail can induce, in the long-term, specific brain adaptations and activate P450 metabolic, or detoxification, pathways. These results require further mechanistic and molecular investigations to explore the causal link existing between a life-long exposure to pesticides and the development of susceptibility-related health elements within the brain-periphery axis.

Table 1. Characteristics and tolerable daily intake (TDI) of each pesticide. Expected and measured pesticide concentrations (µg/kg food) in the food pellet. Adapted from (Lukowicz et al., 2018).

Pesticide name	Chemical family	Function	TDI (mg/kg BW/day)	Expected quantity (µg / kg food)[a]	Measured level (µg / kg food)
Ziram	Dithiocarbamate	Fungicide	0.006	36	ND[b]
Chlorpyrifos	Organophosphorus	Insecticide	0.01	60	47
Thiacloprid	Neonicotinoid	Insecticide	0.01	60	56
Boscalid	Carboxamide	Fungicide	0.04	240	240
Thiofanate	Benzimidazole	Fungicide	0.08	480	205
Captan	Dicarboximide	Fungicide	0.1	600	165

Note: BW, Body weight; ND, not determined; TDI, tolerable daily intake (http://www.agritox.anses.fr/).
[a]Expected quantity refers to the incorporated quantities of pesticides in mice pellets.
[b]Ziram was not at detectible level (<0.01mg/kg).

Figure legends

Figure 1. Spatio-temporally delimited hippocampal astrogliosis during pesticides exposure in the long term. A1-A4) Examples of GFAP and DAPI immunostaining in the CA1 regions of male and female mice at 12 months. Examples of reactive astrocytes in the parenchyma and perivascular are indicated in A2 (*arrowheads* and *lines*). **B1-B2, C1-C2)** Quantification of percentage GFAP fluorescence in the sub-hippocampal regions. **D1-D2)** Analysis of GFAP immunoreactivity in the neocortex. Each dot represents the quantitation from one brain slice. Number of mice / group: i) n=8 pesticide diet, n=8 standard diet male mice at 3 months; ii) n=7 pesticide diet; n=8 standard diet female mice at 3 months; iii) n=8 pesticide diet, n=8 standard diet male mice; iv) n=8 pesticide diet, n=8 standard diet female mice at 12 months. One or two brain slices / mouse were used. Data are analyzed using non-parametric Kruskal-Willis ANOVA and Dunn's multiple comparisons test: (**B1**) H_3=36.02, p<0.0001, (**B2**) H_3=37.20, p<0.0001, (**C1**) H_3=21.93, p<0.0001, (**C2**) H_3= 34.61, p<0.0001, (**D1**) H_3= 21.36, p<0.0001, (**D2**) H_3= 15.44, p = 0.015. The Dunn's test was used for multiple comparisons between groups: * p<0.05, ** p<0.01 and *** p<0.001 (as reported in the figure).

Figure 2. Pattern of PDGFRβ brain expression during long-term pesticide exposure. (A1-A4, B1-B4) Examples of PDGFRβ and cerebrovascular IsoB4 immunostaining in the CA1 region and fronto-parietal neocortex of male and female mice at 12 months. *Arrowheads* indicate parenchymal cells and perivascular PDGFRβ reactivity in the pesticide exposed groups. *Asterisks* indicate capillary pericytes. **(C1-C2, D1-D2)** Quantification of PDGFRβ fluorescence normalized by IsoB4 in the sub-hippocampal regions. **(E1-E2)** Analysis of cortical PDGFRβ immunoreactivity. Number of mice / group: i) n=8 pesticide diet, n=8 standard diet male mice at 3 months; ii) n=7 pesticide diet; n=8 standard diet female mice at 3 months; iii) n=8 pesticide diet, n=8 standard diet male mice; iv) n=8 pesticide diet, n=8 standard diet female mice at 12 months. One or two brain slices / mouse were used. Data are analyzed using non-parametric Kruskal-Willis ANOVA and Dunn's multiple comparisons test: (**C1**) H_3= 16.95, p = 0.0007, (**C2)** H_3= 27.22, p<0.0001, (**D1**) H_3= 8.208, p = 0.042, (**D2**) H_3= 23.13, p<0.0001, (**E1**) H_3= 22.64, p<0.0001,

(**E2**) H_3= 29.78, p<0.0001. The Dunn's test was used for multiple comparisons between groups: * p<0.05, ** p<0.01 and *** p<0.001 (as reported in the figure).

Figure 3. Dietary exposure to pesticides promotes distinct behavioral impairments in males. (**A**) body weight (g); (**B**) spontaneous alternation behavior (%) and (**C**) total number of arm entries in the Y-maze; (**D**) time spent interacting during the social interaction test; (**E**) locomotor activity (distance in cm) in the open field; anxiety-like behaviors in 3 and 12 months control and pesticides-exposed mice, including time spent in the center zone of the open field (**F**), in the light zone of the light/dark transition apparatus (**G**) and in the open arms of the EPM (**H**). Number of mice per group: control males 3-12 months (n=9), pesticides males 3-12 months (n=10). Data are analyzed using the non-parametric Kruskal-Willis ANOVA: (**A**) H_3=26.62, p<0.0001, (**B**) H_3=10.92, p=0.0122, (**C**) H_3=2.34, p=0.5048, (**D**) H_3=23.52, p<0.0001, (**E**) H_3=12.62, p=0.0055, (**F**) H_3=20.66, p<0.0001, (**G**) H_3=3.011, p=0.3899, (**H**) H_3=6.509, p=0.0893. The Dunn's test was used for multiple comparisons between groups: * p<0.05, ** p<0.01 and *** p<0.001 (as reported in the figure).

Figure 4. Dietary exposure to pesticides does not promote behavioral impairments in females. (**A**) body weight (g); (**B**) spontaneous alternation behavior (%) and (**C**) total number of arm entries in the Y-maze; (**D**) time spent interacting during the social interaction test; (**E**) locomotor activity (distance in cm) in the open field; anxiety-like behaviors in 3 and 12 months control and pesticides-exposed mice, including time spent in the center zone of the open field (**F**), in the light zone of the light/dark transition apparatus (**G**) and in the open arms of the EPM (**H**). Number of mice per group: control females 3-12 months (n=10), pesticides females 3-12 months (n=9). Data are analyzed using the non-parametric Kruskal-Willis ANOVA: (**A**) H_3=29.09, p<0.0001, (**B**) H_3=6.05, p=0.1092, (**C**) H_3=4.632, p=0.2009, (**D**) H_3=6.693, p=0.0824, (**E**) H_3=7.027, p=0.0710, (**F**) H_3=11.56, p=0.0091, (**G**) H_3=7.43, p=0.0594, (**H**) H_3=1.717, p=0.6332. The Dunn's test was used for multiple comparisons between groups: * p<0.05 and ** p<0.01 (as reported in the figure).

Figure 5. Outcome of electroencephalographic telemetry explorations during pesticides exposure. **A1-A4)** Examples of EEG traces and color-coded waves distributions (mo: months). Pathological spike or seizure activity were not detected in these experimental conditions. **B1-B4)** Entire frequency spectrograms (0.5 – 80 Hz) for each individual mouse analyzed (blue line: control; red line: pesticide). Each line corresponds to one individual mouse. **C1-C4; D1-D4)** Example of percentage distributions of specific theta and gamma wave ranges in mice at 3 and 12 months during pesticides exposure.

Figure 6. Exposure to pesticides leads to the up-regulation of key cytochromes in the liver. Hepatic P450 cytochromes (Cyp) expression levels were assessed by qPCR. Typical Cyp that are controlled by nuclear the receptors PPARα (**A1-A4:** *Cyp4a14, Cyp4a10*), CAR (**B1-B4**: *Cyp2b10, Cyp2c29*) and PXR (**C1-C4:** *Cyp2c55, Cyp3a11*) were quantified by qPCR in liver at 3 months (n=6) and 12 months of pesticides exposure (n=8). Data are analyzed using the non-parametric Kruskal-Wallis ANOVA: (**A1**) H_3=22,58, p<0.0001, (**A2**) H_3=22,35, p<0.0001, (**A3**) H_3=18,22, p=0,0004, (**A4**) H_3=14,71, p=0,0021, (**B1**) H_3=11,61, p=0,0088, (**B2**) H_3=6,180, p=0,1032, (**B3**) H_3=5,696, p=0,1274, (**B4**) H_3=4,092, p=0,2517, (**C1**) H_3=12,34, p=0,0063, (**C2**) H_3=13,14, p=0,0044, (**C3**) H_3=13,66, p=0,0034, (**C4**) H_3=9,629, p=0,0220. The Dunn's test was used for multiple comparisons between groups: * p<0.05, ** p<0.01 and *** p<0.001 (as reported in the figure).

Figure 7. Exposure to pesticides increases metabolic β-oxydation and lipid transport in the liver. Hepatic gene levels involved in metabolic pathways such as β-oxydation (**A1-A6**: *Acox1, Cpt1α, Eci*), lipid (**B1, B3:** *Cd36*) and glucose (**B2, B4:** *Glut2*) transport (**B**) were quantified by qPCR in liver at 3 months (n=6) and at 12 months of exposure (n=8). Data are analyzed using the non-parametric Kruskal-Wallis ANOVA: (**A1**) H_3=22,02, p<0.0001, (**A2**) H_3=17,02, p=0.0007, (**A3**) H_3=13,72, p=0,0033, (**A4**) H_3=3,645, p=0,3024, (**A5**) H_3=20,66, p=0,0001, (**A6**) H_3=14,36, p=0,0001, (**C1**) H_3=19,75, p=0,0002, (**C2**) H_3=6,190, p=0,1027, (**C3**) H_3=17,57, p=0,0005, (**C4**) H_3=5,107, p=0,1641. The Dunn's test was used for multiple comparisons between groups: * p<0.05, ** p<0.01 and *** p<0.001 (as reported in the figure).

Figure 8. Exposure to pesticides leads to the up-regulation of P450 cytochromes in kidneys. Renal P450 cytochromes (Cyp) expression levels were assessed by qPCR. Typical Cyp that are controlled by nuclear the receptors PPARα (**A1-A2**: *Cyp4a14, Cyp4a10*), CAR (**B1-B2**: *Cyp2b10, Cyp2c29*) and PXR (**C1-C2:** *Cyp2c55, Cyp3a11*) were quantified in kidneys at 12 months of exposure (n=8). Data are analyzed using the non-parametric Kruskal-Wallis ANOVA: (**A1**) H_3=23,06, p<0.0001, (**A2**) H_3=21,84, p<0,0001, (**B1**) H_3=19,93, p=0,0002, (**B2**) H_3=5,477, p=0,1400, (**C1**) H_3=17,38, p=0,0006, (**C2**) H_3=16,45, p=0,0009. The Dunn's test was used for multiple comparisons between groups: * p<0.05, ** p<0.01 and *** p<0.001 (as reported in the figure).

Oligonucleotide sequences

Gene	Ref GenBank	Forward primer (5'-3')	Reverse primer (3'-5')
Cyp2b10	NM_009999	TTTCTGCCCTTCTCAACAGGAA	ATGGACGTGAAGAAAAGGAACAAC
Cyp2c29	NM_007815	GCTCAAAGCCTACTGTCA	CATGAGTGTAAATCGTCTCA
Cyp2c55	NM_028089.3	TTGTGGAAGAGCTAAGAAAAGCAAAT	GAGCACAGCTCAGGATGAATGT
Cyp3a11	NM_007818	TCACACACACAGTTGTAGGCAGAA	GTTTACGAGTCCCATATCGGTAGAG
Cyp4a14	NM_007822	TCAGTCTATTTCTGGTGCTGTTC	GAGCTCCTTGTCCTTCAGATGGT
Cyp4a10	NM_010011	ATTAGTGAGAGTGAGGACAGCAACAG	CCAACCCGATTTGCAGACA
Acox1	NM_015729	CAGACCCTGAAGAAATCATGTGG	CAGGAACATGCCCAAGTGAAG
Cpt1α	NM_013495	GAAGAAGAAGTTCATCCGATTCAAG	GATATCACACCCACCACCACG
Eci	NM_010023	GTTCACCATCAGCCTGGAGAAG	AGAAGATACCCGGGCATTCC
Cd36	NM_007643	GTTAAACAAAGAGGTCCTTACACATACAG	CAGTGAAGGCTCAAAGATGGC
Glut2	NM_031197	TTTGCAGTGGGCGGAATGG	GCCAACATTGCTTTGATCCTT

Reference

Abass K, Lamsa V, Reponen P, Kublbeck J, Honkakoski P, Mattila S, Pelkonen O, Hakkola J (2012) Characterization of human cytochrome P450 induction by pesticides. Toxicology 294: 17-26.

Ait-Bali Y, Ba-M'hamed S, Gambarotta G, Sassoe-Pognetto M, Giustetto M, Bennis M (2020) Pre- and postnatal exposure to glyphosate-based herbicide causes behavioral and cognitive impairments in adult mice: evidence of cortical ad hippocampal dysfunction. Arch Toxicol DOI 10.1007/s00204-020-02677-7.

Al-Eryani L, Wahlang B, Falkner KC, Guardiola JJ, Clair HB, Prough RA, Cave M (2015) Identification of Environmental Chemicals Associated with the Development of Toxicant-associated Fatty Liver Disease in Rodents. Toxicol Pathol 43: 482-497.

Azcoitia I, Santos-Galindo M, Arevalo MA, Garcia-Segura LM (2010) Role of astroglia in the neuroplastic and neuroprotective actions of estradiol. Eur J Neurosci 32: 1995-2002.

Banks CN, Lein PJ (2012) A review of experimental evidence linking neurotoxic organophosphorus compounds and inflammation. Neurotoxicology 33: 575-584.

Bogush M, Heldt NA, Persidsky Y (2017) Blood Brain Barrier Injury in Diabetes: Unrecognized Effects on Brain and Cognition. J Neuroimmune Pharmacol 12: 593-601.

Boussadia B, Gangarossa G, Mselli-Lakhal L, Rousset MC, de Bock F, Lassere F, Ghosh C, Pascussi JM, Janigro D, Marchi N (2016) Lack of CAR impacts neuronal function and cerebrovascular integrity in vivo. Exp Neurol 283: 39-48.

Boussadia B, Lakhal L, Payrastre L, Ghosh C, Pascussi JM, Gangarossa G, Marchi N (2018) Pregnane X Receptor Deletion Modifies Recognition Memory and Electroencephalographic Activity. Neuroscience 370: 130-138.

Casals-Casas C, Desvergne B (2011) Endocrine disruptors: from endocrine to metabolic disruption. Annu Rev Physiol 73: 135-162.

Czajka M, Matysiak-Kucharek M, Jodlowska-Jedrych B, Sawicki K, Fal B, Drop B, Kruszewski M, Kapka-Skrzypczak L (2019) Organophosphorus pesticides can influence the development of obesity and type 2 diabetes with concomitant metabolic changes. Environ Res 178: 108685.

Dallerac G, Rouach N (2016) Astrocytes as new targets to improve cognitive functions. Prog Neurobiol 144: 48-67.

De Long NE, Holloway AC (2017) Early-life chemical exposures and risk of metabolic syndrome. Diabetes Metab Syndr Obes 10: 101-109.

Deitmer JW, Theparambil SM, Ruminot I, Noor SI, Becker HM (2019) Energy Dynamics in the Brain: Contributions of Astrocytes to Metabolism and pH Homeostasis. Front Neurosci 13: 1301.

Donovan JP, Schafer DF, Shaw BW, Jr., Sorrell MF (1998) Cerebral oedema and increased intracranial pressure in chronic liver disease. Lancet 351: 719-721.

dos Santos AA, Naime AA, de Oliveira J, Colle D, dos Santos DB, Hort MA, Moreira EL, Sunol C, de Bem AF, Farina M (2016) Long-term and low-dose malathion exposure causes cognitive impairment in adult mice: evidence of hippocampal mitochondrial dysfunction, astrogliosis and apoptotic events. Arch Toxicol 90: 647-660.

Evangelou E, Ntritsos G, Chondrogiorgi M, Kavvoura FK, Hernandez AF, Ntzani EE, Tzoulaki I (2016) Exposure to pesticides and diabetes: A systematic review and meta-analysis. Environ Int 91: 60-68.

Ferguson CS, Tyndale RF (2011) Cytochrome P450 enzymes in the brain: emerging evidence of biological significance. Trends Pharmacol Sci 32: 708-714.
Gangemi S, Gofita E, Costa C, Teodoro M, Briguglio G, Nikitovic D, Tzanakakis G, Tsatsakis AM, Wilks MF, Spandidos DA, Fenga C (2016) Occupational and environmental exposure to pesticides and cytokine pathways in chronic diseases (Review). Int J Mol Med 38: 1012-1020.
Ghosh C, Puvenna V, Gonzalez-Martinez J, Janigro D, Marchi N (2011) Blood-brain barrier P450 enzymes and multidrug transporters in drug resistance: a synergistic role in neurological diseases. Curr Drug Metab 12: 742-749.
Giannoni P, Claeysen S, Noe F, Marchi N (2020) Peripheral Routes to Neurodegeneration: Passing Through the Blood-Brain Barrier. Front Aging Neurosci 12: 3.
Guillemot-Legris O, Muccioli GG (2017) Obesity-Induced Neuroinflammation: Beyond the Hypothalamus. Trends Neurosci 40: 237-253.
Hernandez AF, Gonzalez-Alzaga B, Lopez-Flores I, Lacasana M (2016) Systematic reviews on neurodevelopmental and neurodegenerative disorders linked to pesticide exposure: Methodological features and impact on risk assessment. Environ Int 92-93: 657-679.
Iaccarino HF, Singer AC, Martorell AJ, Rudenko A, Gao F, Gillingham TZ, Mathys H, Seo J, Kritskiy O, Abdurrob F, Adaikkan C, Canter RG, Rueda R, Brown EN, Boyden ES, Tsai LH (2018) Author Correction: Gamma frequency entrainment attenuates amyloid load and modifies microglia. Nature 562: E1.
Ichkova A, Rodriguez-Grande B, Zub E, Saudi A, Fournier ML, Aussudre J, Sicard P, Obenaus A, Marchi N, Badaut J (2020) Early cerebrovascular and long-term neurological modifications ensue following juvenile mild traumatic brain injury in male mice. Neurobiol Dis 141: 104952.
Jaber SM, Bordt EA, Bhatt NM, Lewis DM, Gerecht S, Fiskum G, Polster BM (2018) Sex differences in the mitochondrial bioenergetics of astrocytes but not microglia at a physiologically relevant brain oxygen tension. Neurochem Int 117: 82-90.
Kamel F, Hoppin JA (2004) Association of pesticide exposure with neurologic dysfunction and disease. Environ Health Perspect 112: 950-958.
Kitchigina VF (2018) Alterations of Coherent Theta and Gamma Network Oscillations as an Early Biomarker of Temporal Lobe Epilepsy and Alzheimer's Disease. Front Integr Neurosci 12: 36.
Klement W, Blaquiere M, Zub E, deBock F, Boux F, Barbier E, Audinat E, Lerner-Natoli M, Marchi N (2019) A pericyte-glia scarring develops at the leaky capillaries in the hippocampus during seizure activity. Epilepsia 60: 1399-1411.
Kyyriainen J, Ekolle Ndode-Ekane X, Pitkanen A (2017) Dynamics of PDGFRbeta expression in different cell types after brain injury. Glia 65: 322-341.
Li JT, Xie XM, Yu JY, Sun YX, Liao XM, Wang XX, Su YA, Liu YJ, Schmidt MV, Wang XD, Si TM (2017) Suppressed Calbindin Levels in Hippocampal Excitatory Neurons Mediate Stress-Induced Memory Loss. Cell Rep 21: 891-900.
Li Q, Barres BA (2018) Microglia and macrophages in brain homeostasis and disease. Nat Rev Immunol 18: 225-242.
Lim KL, Tay A, Nadarajah VD, Mitra NK (2011) The effect of consequent exposure of stress and dermal application of low doses of chlorpyrifos on the expression of glial fibrillary acidic protein in the hippocampus of adult mice. J Occup Med Toxicol 6: 4.
Lukowicz C, Ellero-Simatos S, Regnier M, Polizzi A, Lasserre F, Montagner A, Lippi Y, Jamin EL, Martin JF, Naylies C, Canlet C, Debrauwer L, Bertrand-Michel J, Al Saati T, Theodorou V, Loiseau N, Mselli-Lakhal L, Guillou H, Gamet-Payrastre L

(2018) Metabolic Effects of a Chronic Dietary Exposure to a Low-Dose Pesticide Cocktail in Mice: Sexual Dimorphism and Role of the Constitutive Androstane Receptor. Environ Health Perspect 126: 067007.
Lushchak VI, Matviishyn TM, Husak VV, Storey JM, Storey KB (2018) Pesticide toxicity: a mechanistic approach. EXCLI J 17: 1101-1136.
Mably AJ, Colgin LL (2018) Gamma oscillations in cognitive disorders. Curr Opin Neurobiol 52: 182-187.
Miller AA, Spencer SJ (2014) Obesity and neuroinflammation: a pathway to cognitive impairment. Brain Behav Immun 42: 10-21.
Morita M, Ikeshima-Kataoka H, Kreft M, Vardjan N, Zorec R, Noda M (2019) Metabolic Plasticity of Astrocytes and Aging of the Brain. Int J Mol Sci 20.
Morrison HW, Filosa JA (2016) Sex differences in astrocyte and microglia responses immediately following middle cerebral artery occlusion in adult mice. Neuroscience 339: 85-99.
Mouton PR, Long JM, Lei DL, Howard V, Jucker M, Calhoun ME, Ingram DK (2002) Age and gender effects on microglia and astrocyte numbers in brains of mice. Brain Res 956: 30-35.
Nasr HM, El-Demerdash FM, El-Nagar WA (2016) Neuro and renal toxicity induced by chlorpyrifos and abamectin in rats: Toxicity of insecticide mixture. Environ Sci Pollut Res Int 23: 1852-1859.
Nisbett KE, Pinna G (2018) Emerging Therapeutic Role of PPAR-alpha in Cognition and Emotions. Front Pharmacol 9: 998.
Ojo JO, Abdullah L, Evans J, Reed JM, Montague H, Mullan MJ, Crawford FC (2014) Exposure to an organophosphate pesticide, individually or in combination with other Gulf War agents, impairs synaptic integrity and neuronal differentiation, and is accompanied by subtle microvascular injury in a mouse model of Gulf War agent exposure. Neuropathology 34: 109-127.
Pekny M, Pekna M, Messing A, Steinhauser C, Lee JM, Parpura V, Hol EM, Sofroniew MV, Verkhratsky A (2016) Astrocytes: a central element in neurological diseases. Acta Neuropathol 131: 323-345.
Pu Y, Yang J, Chang L, Qu Y, Wang S, Zhang K, Xiong Z, Zhang J, Tan Y, Wang X, Fujita Y, Ishima T, Wang D, Hwang SH, Hammock BD, Hashimoto K (2020) Maternal glyphosate exposure causes autism-like behaviors in offspring through increased expression of soluble epoxide hydrolase. Proc Natl Acad Sci U S A 117: 11753-11759.
Riew TR, Choi JH, Kim HL, Jin X, Lee MY (2018) PDGFR-beta-Positive Perivascular Adventitial Cells Expressing Nestin Contribute to Fibrotic Scar Formation in the Striatum of 3-NP Intoxicated Rats. Front Mol Neurosci 11: 402.
Rom S, Zuluaga-Ramirez V, Gajghate S, Seliga A, Winfield M, Heldt NA, Kolpakov MA, Bashkirova YV, Sabri AK, Persidsky Y (2019) Hyperglycemia-Driven Neuroinflammation Compromises BBB Leading to Memory Loss in Both Diabetes Mellitus (DM) Type 1 and Type 2 Mouse Models. Mol Neurobiol 56: 1883-1896.
Runtz L, Girard B, Toussenot M, Espallergues J, Fayd'Herbe De Maudave A, Milman A, deBock F, Ghosh C, Guerineau NC, Pascussi JM, Bertaso F, Marchi N (2018) Hepatic and hippocampal cytochrome P450 enzyme overexpression during spontaneous recurrent seizures. Epilepsia 59: 123-134.
Santos-Galindo M, Acaz-Fonseca E, Bellini MJ, Garcia-Segura LM (2011) Sex differences in the inflammatory response of primary astrocytes to lipopolysaccharide. Biol Sex Differ 2: 7.
Sofroniew MV (2014) Astrogliosis. Cold Spring Harb Perspect Biol 7: a020420.

Stevenson EL, Caldwell HK (2014) Lesions to the CA2 region of the hippocampus impair social memory in mice. Eur J Neurosci 40: 3294-3301.
Sureka B, Bansal K, Patidar Y, Rajesh S, Mukund A, Arora A (2015) Neurologic Manifestations of Chronic Liver Disease and Liver Cirrhosis. Curr Probl Diagn Radiol 44: 449-461.
Suzuki A, Stern SA, Bozdagi O, Huntley GW, Walker RH, Magistretti PJ, Alberini CM (2011) Astrocyte-neuron lactate transport is required for long-term memory formation. Cell 144: 810-823.
Tassoni A, Farkhondeh V, Itoh Y, Itoh N, Sofroniew MV, Voskuhl RR (2019) The astrocyte transcriptome in EAE optic neuritis shows complement activation and reveals a sex difference in astrocytic C3 expression. Sci Rep 9: 10010.
Wang P, Wang HP, Xu MY, Liang YJ, Sun YJ, Yang L, Li L, Li W, Wu YJ (2014) Combined subchronic toxicity of dichlorvos with malathion or pirimicarb in mice liver and serum: a metabonomic study. Food Chem Toxicol 70: 222-230.
Zurich MG, Honegger P, Schilter B, Costa LG, Monnet-Tschudi F (2004) Involvement of glial cells in the neurotoxicity of parathion and chlorpyrifos. Toxicol Appl Pharmacol 201: 97-104.

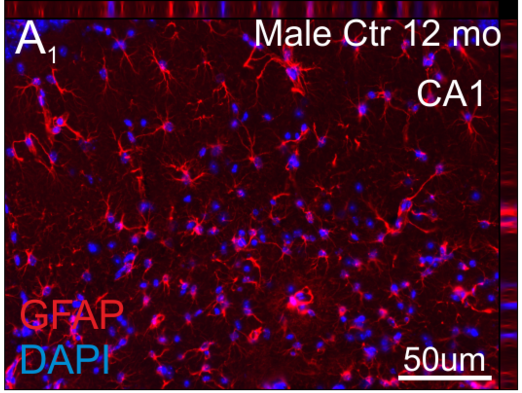
A1
Male Ctr 12 mo
CA1
GFAP
DAPI
50um

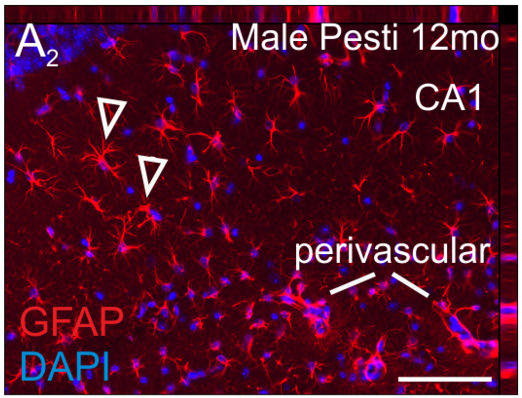
A2
Male Pesti 12mo
CA1
perivascular
GFAP
DAPI

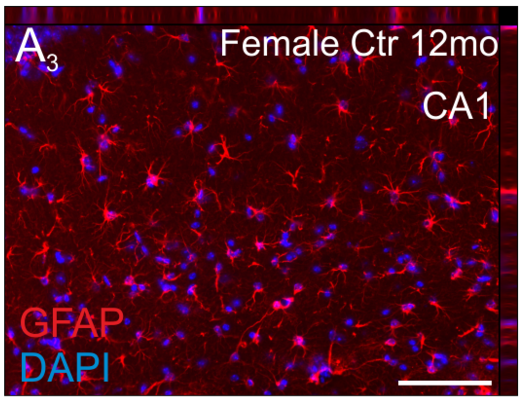
A3
Female Ctr 12mo
CA1
GFAP
DAPI

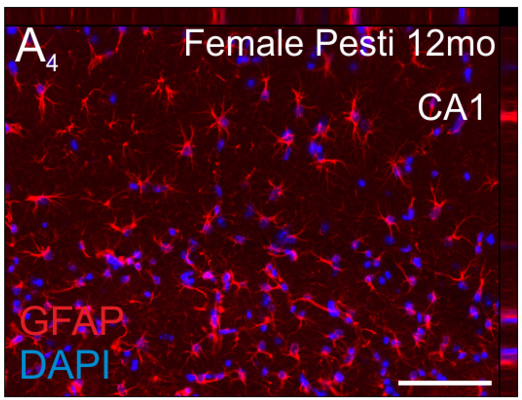
A4
Female Pesti 12mo
CA1
GFAP
DAPI

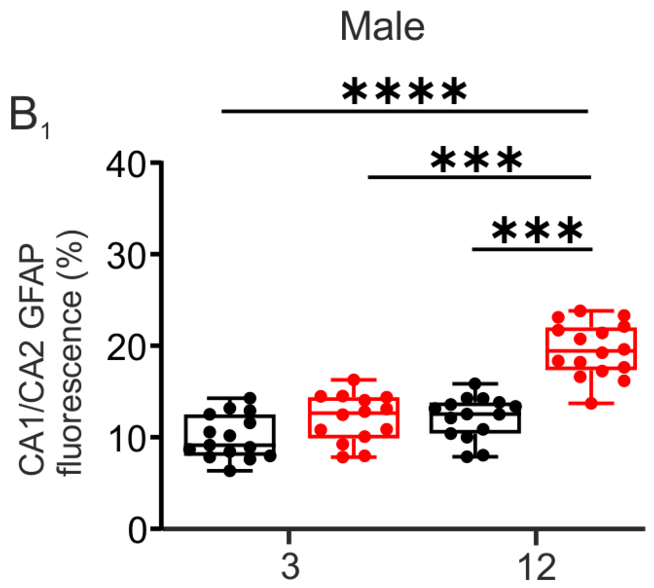
Male
B1
****
***
***
CA1/CA2 GFAP fluorescence (%)
0
10
20
30
40
3
12

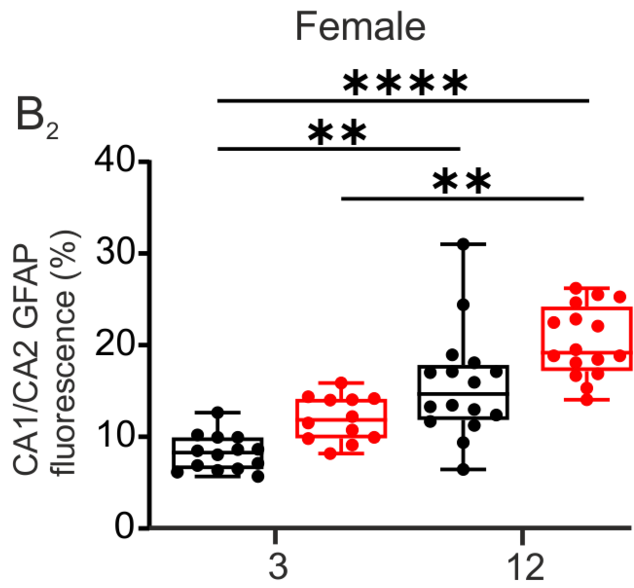
Female
B2
****
**
**
CA1/CA2 GFAP fluorescence (%)
0
10
20
30
40
3
12

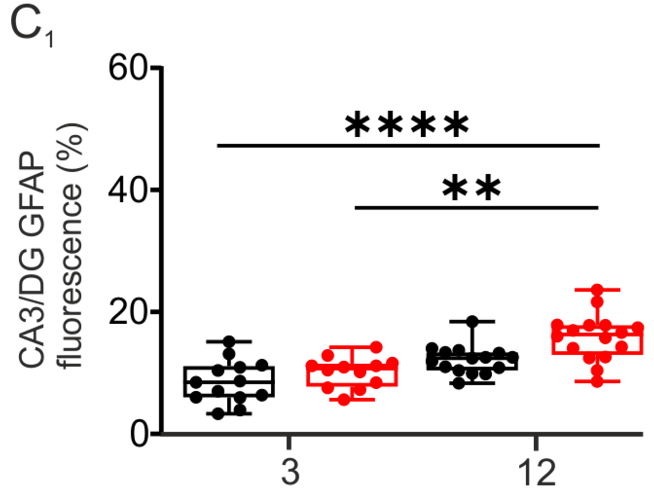
C1
****
**
CA3/DG GFAP fluorescence (%)
0
20
40
60
3
12

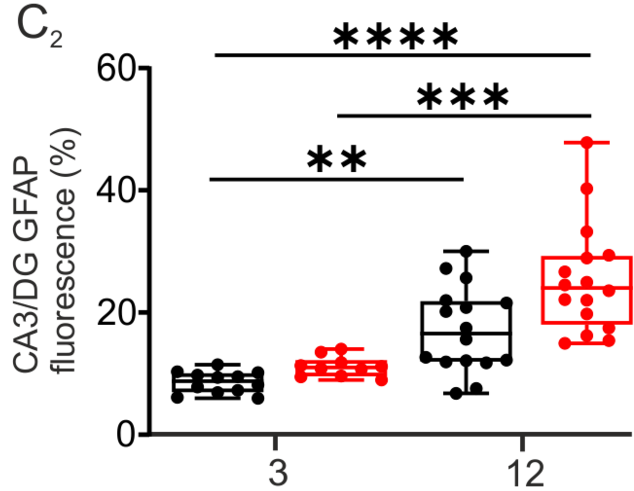
C2
****
***
**
CA3/DG GFAP fluorescence (%)
0
20
40
60
3
12

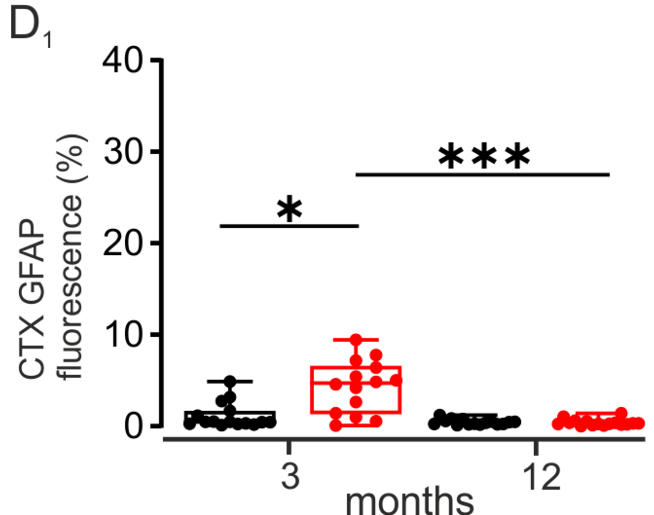
D1
*
***
CTX GFAP fluorescence (%)
0
10
20
30
40
3
12
months

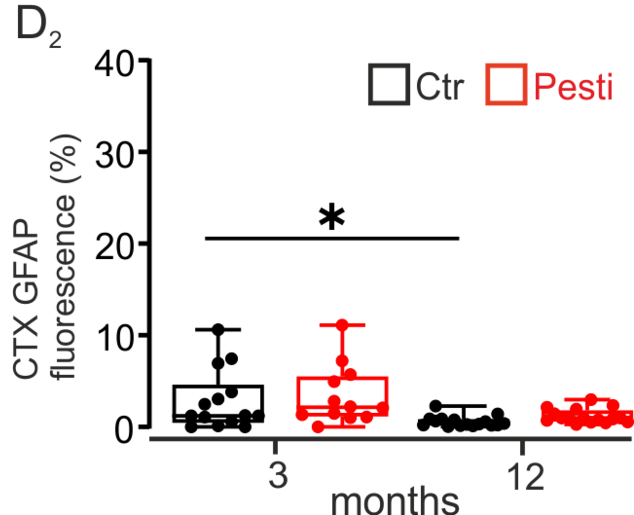
D2
Ctr
Pesti
*
CTX GFAP fluorescence (%)
0
10
20
30
40
3
12
months

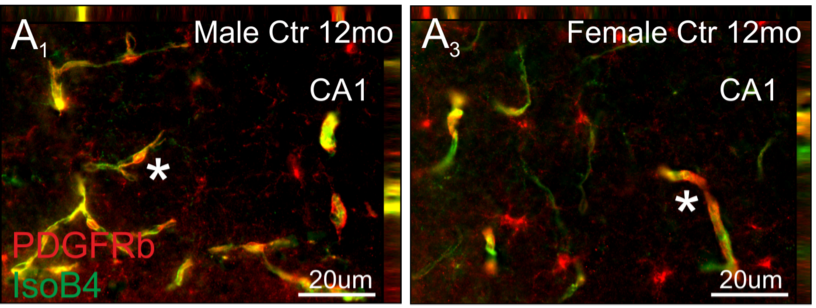
A1
Male Ctr 12mo
CA1
PDGFRb
IsoB4
20um

A3
Female Ctr 12mo
CA1
20um

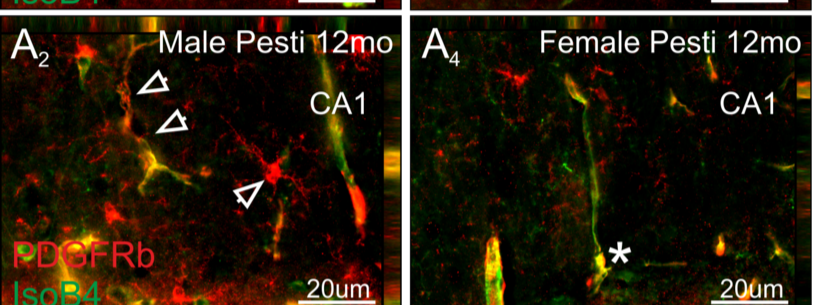
A2
Male Pesti 12mo
CA1
PDGFRb
IsoB4
20um

A4
Female Pesti 12mo
CA1
20um

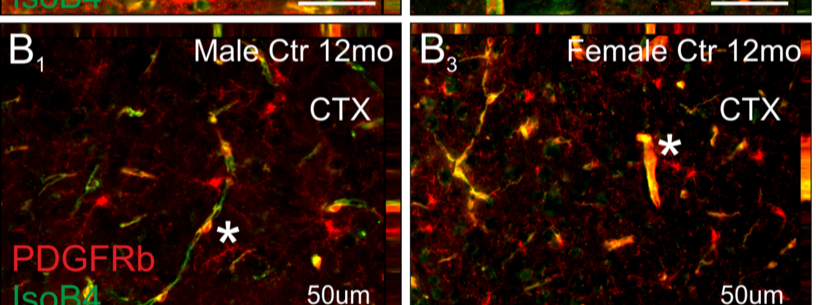
B1
Male Ctr 12mo
CTX
PDGFRb
IsoB4
50um

B3
Female Ctr 12mo
CTX
50um

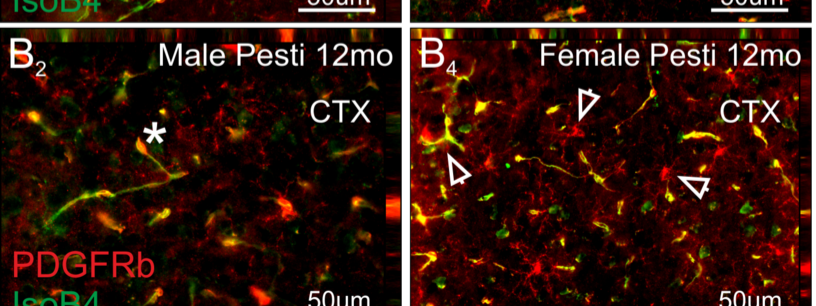
B2
Male Pesti 12mo
CTX
PDGFRb
IsoB4
50um

B4
Female Pesti 12mo
CTX
50um

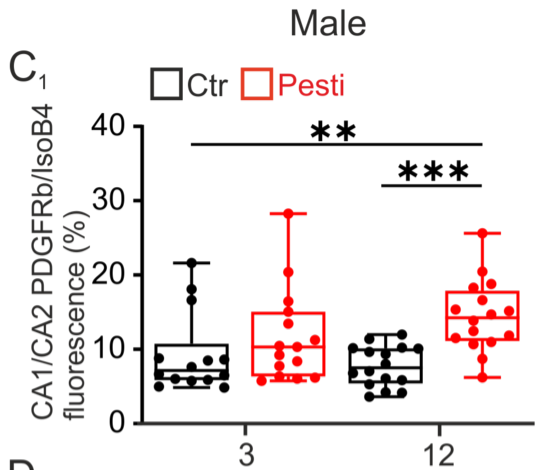
Male
C1
Ctr
Pesti
CA1/CA2 PDGFRb/IsoB4 fluorescence (%)
0
10
20
30
40
3
12
**
***

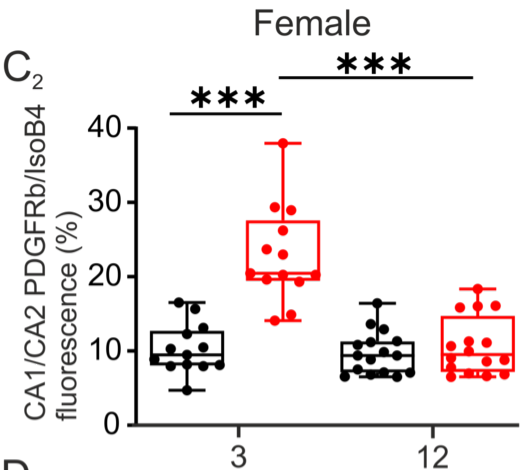
Female
C2
CA1/CA2 PDGFRb/IsoB4 fluorescence (%)
0
10
20
30
40
3
12
***
***

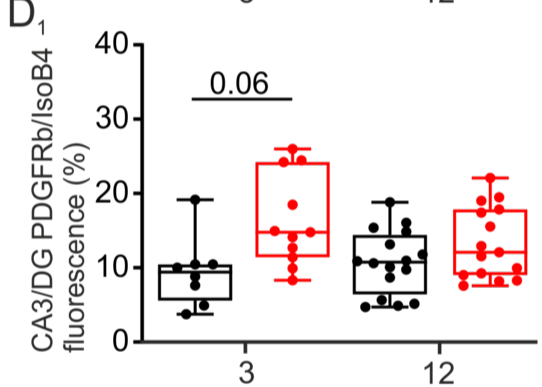
D1
CA3/DG PDGFRb/IsoB4 fluorescence (%)
0
10
20
30
40
3
12
0.06

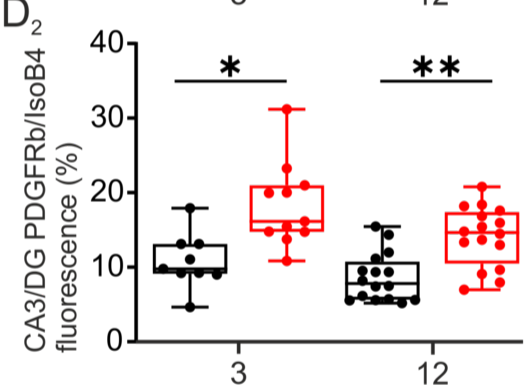
D2
CA3/DG PDGFRb/IsoB4 fluorescence (%)
0
10
20
30
40
3
12
*
**

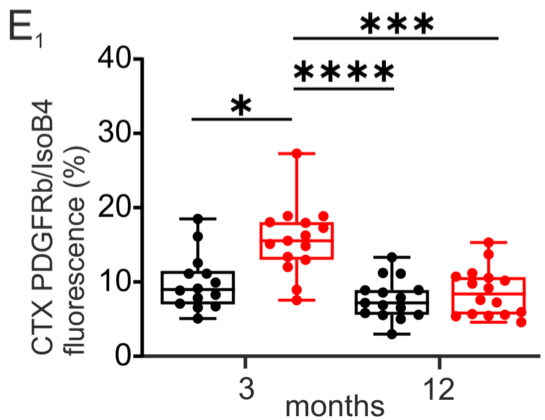
E1
CTX PDGFRb/IsoB4 fluorescence (%)
0
10
20
30
40
3
12
months
*
****
***

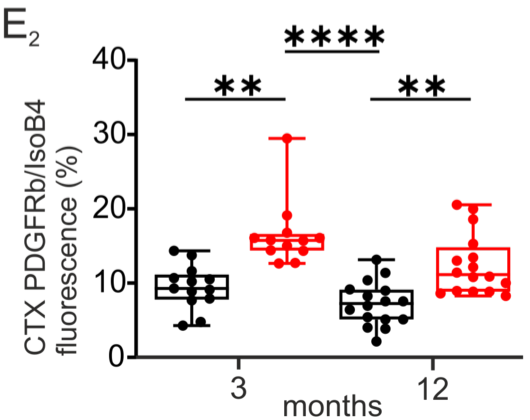
E2
CTX PDGFRb/IsoB4 fluorescence (%)
0
10
20
30
40
3
12
months
**
****
**

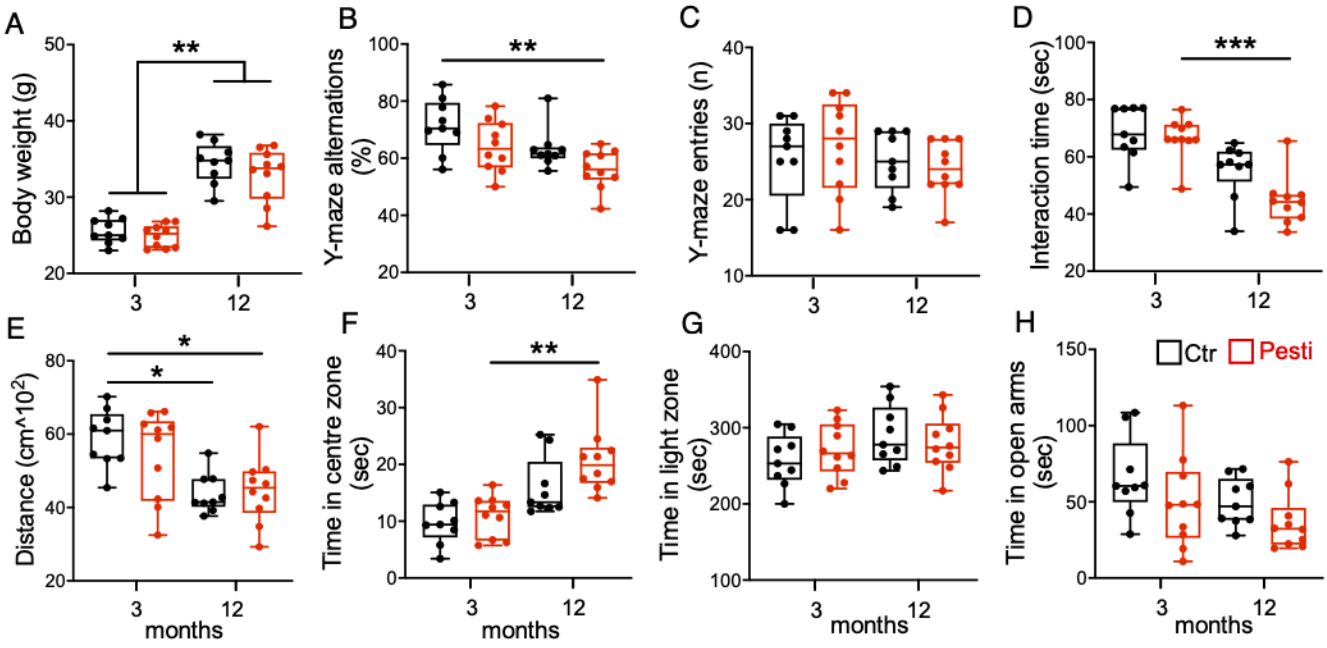
A
Body weight (g)
**
B
Y-maze alternations (%)
**
C
Y-maze entries (n)
D
Interaction time (sec)
***
E
Distance (cm^10^2)
*
*
F
Time in centre zone (sec)
**
G
Time in light zone (sec)
H
Time in open arms (sec)
Ctr
Pesti
3
12
months

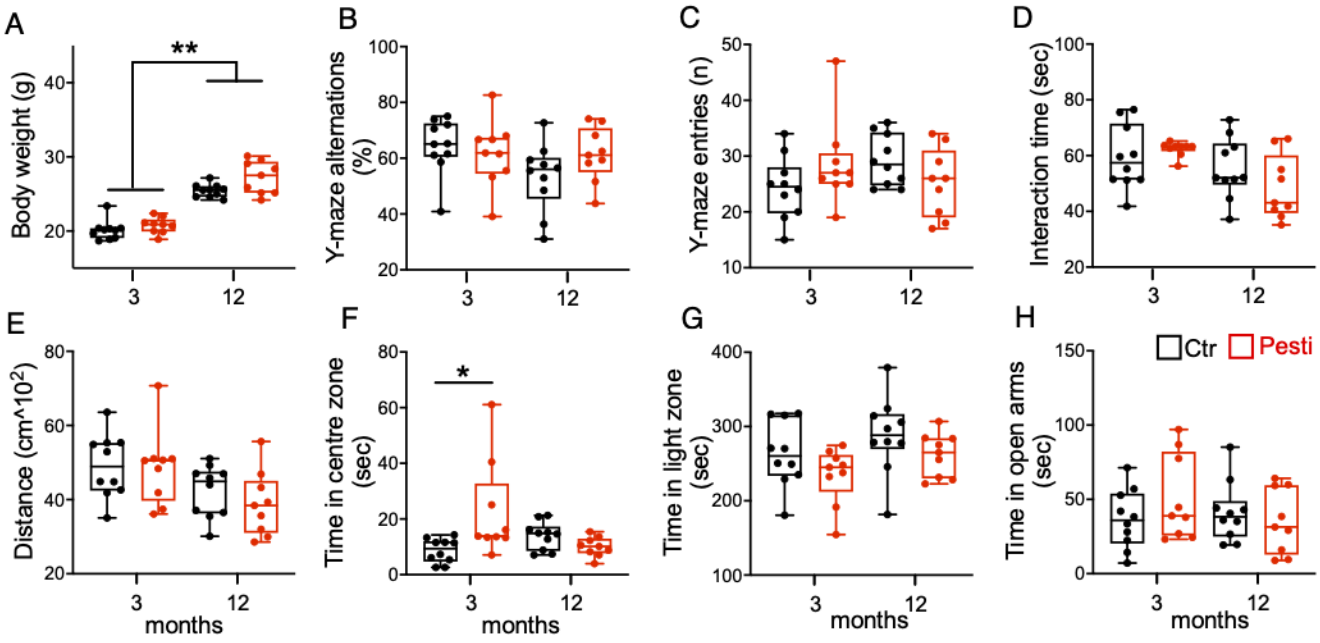
A
Body weight (g)
**
B
Y-maze alternations (%)
C
Y-maze entries (n)
D
Interaction time (sec)
E
Distance (cm^10^2)
months
F
Time in centre zone (sec)
*
months
G
Time in light zone (sec)
months
H
Ctr
Pesti
Time in open arms (sec)
months

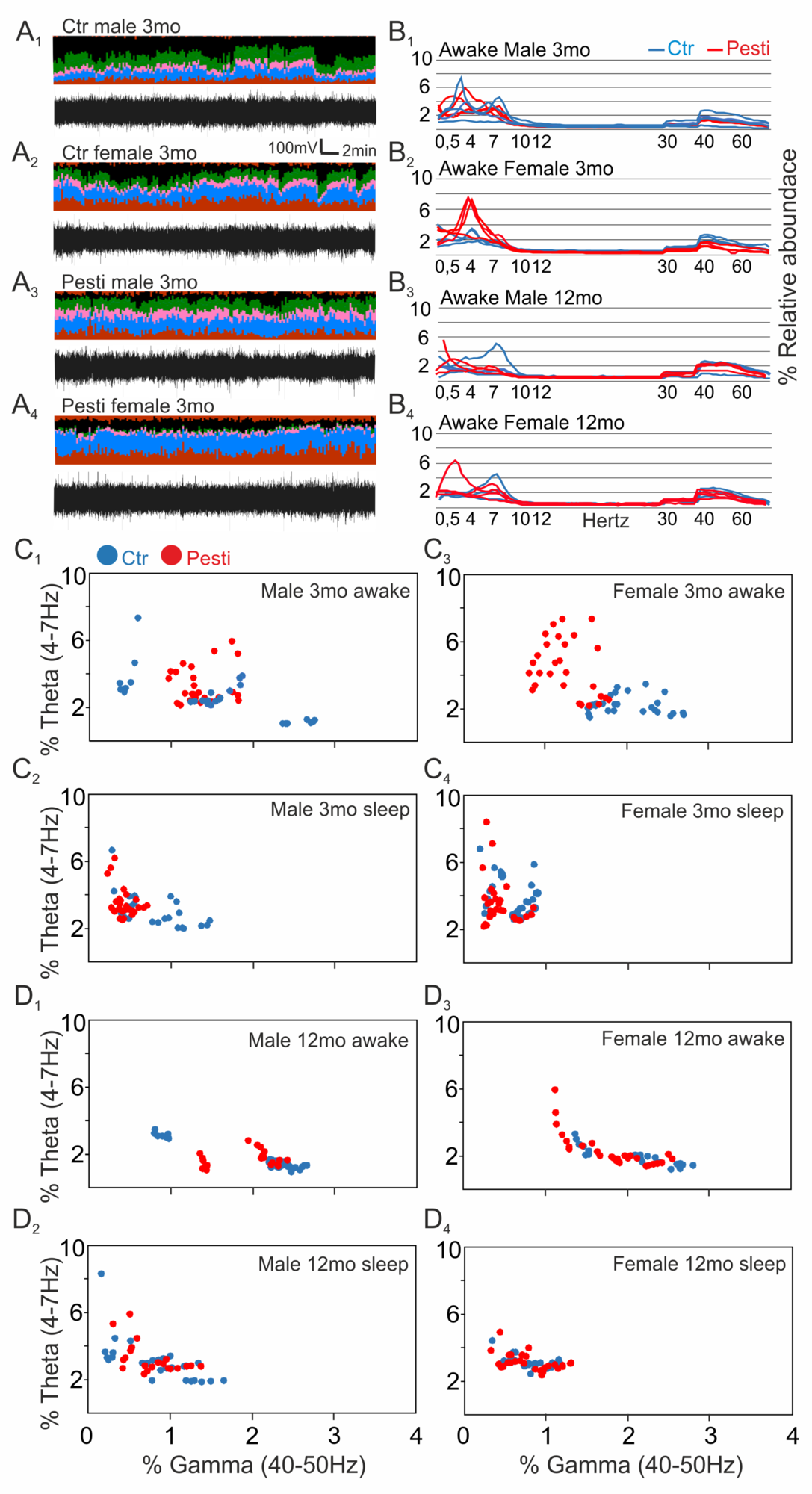
A1
Ctr male 3mo
A2
Ctr female 3mo
100mV
2min
A3
Pesti male 3mo
A4
Pesti female 3mo
B1
Awake Male 3mo
Ctr
Pesti
B2
Awake Female 3mo
B3
Awake Male 12mo
B4
Awake Female 12mo
10
6
2
0,5 4 7 10 12
30 40 60
Hertz
% Relative abondance
C1
Ctr
Pesti
Male 3mo awake
C3
Female 3mo awake
C2
Male 3mo sleep
C4
Female 3mo sleep
D1
Male 12mo awake
D3
Female 12mo awake
D2
Male 12mo sleep
D4
Female 12mo sleep
% Theta (4-7Hz)
0
1
2
3
4
% Gamma (40-50Hz)

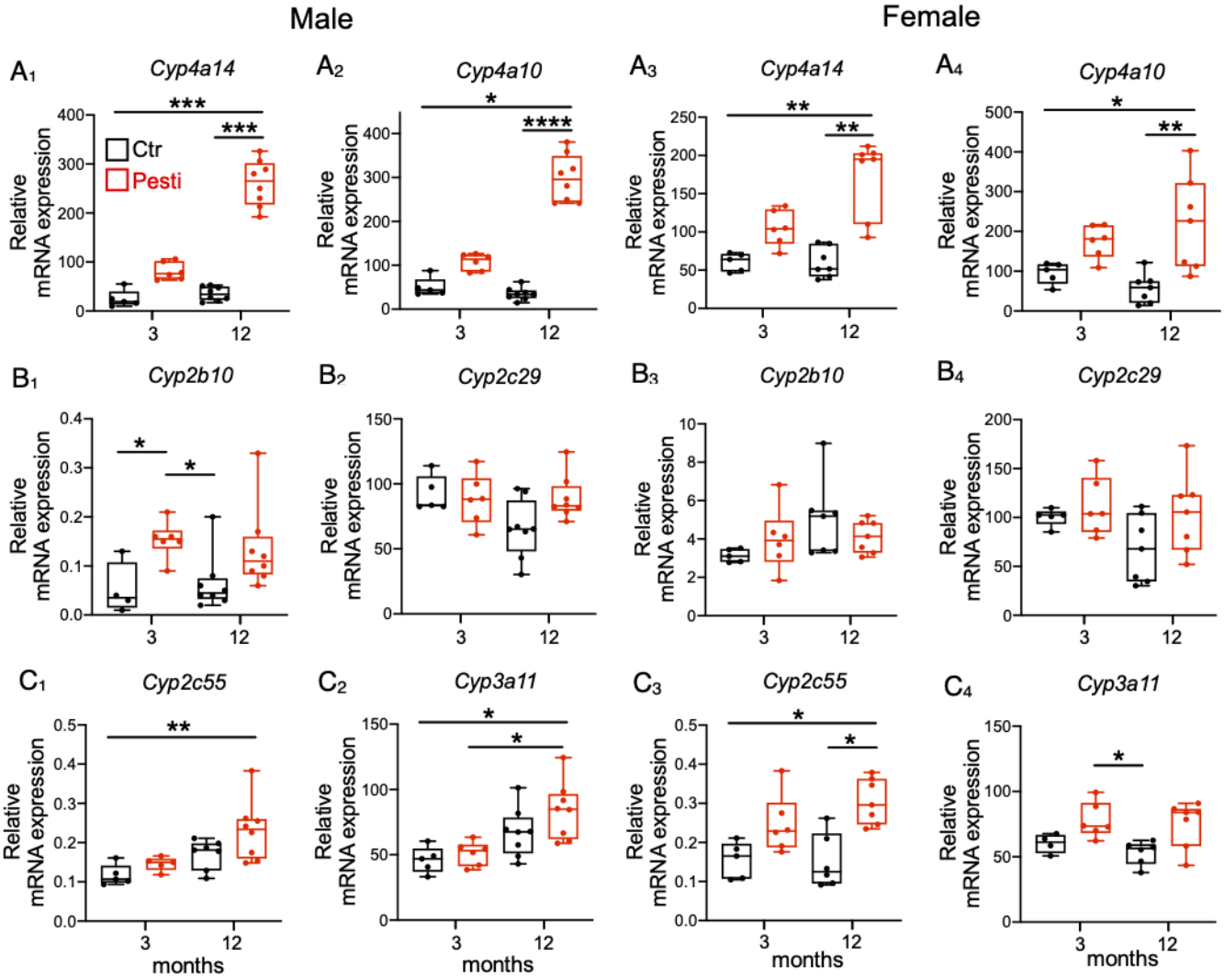
Male
Female
A1
Cyp4a14
A2
Cyp4a10
A3
Cyp4a14
A4
Cyp4a10
B1
Cyp2b10
B2
Cyp2c29
B3
Cyp2b10
B4
Cyp2c29
C1
Cyp2c55
C2
Cyp3a11
C3
Cyp2c55
C4
Cyp3a11
Relative mRNA expression
Ctr
Pesti
months
3
12

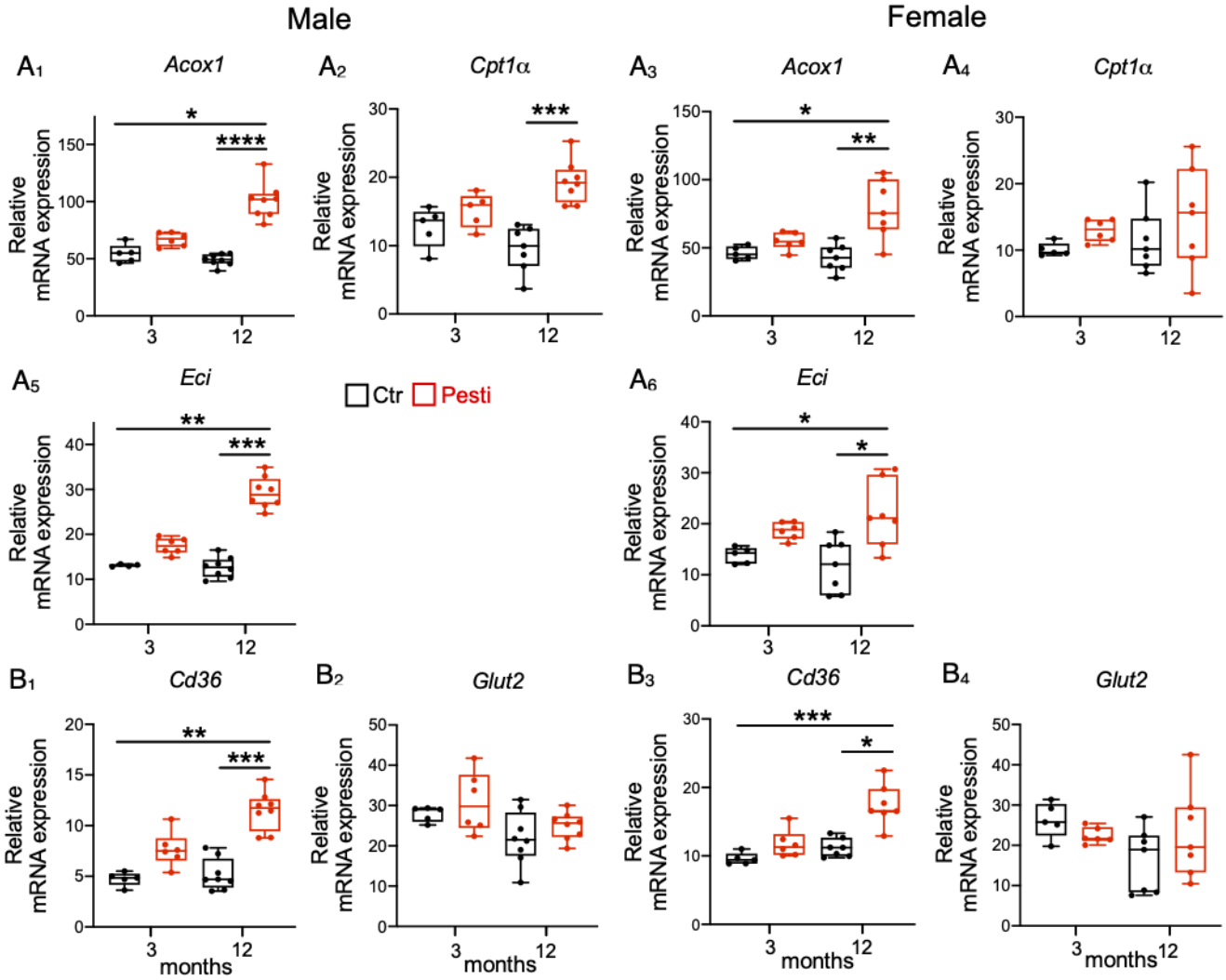
Male
Female
A1
Acox1
A2
Cpt1α
A3
Acox1
A4
Cpt1α
A5
Eci
A6
Eci
Ctr
Pesti
B1
Cd36
B2
Glut2
B3
Cd36
B4
Glut2
Relative mRNA expression
months
3
12

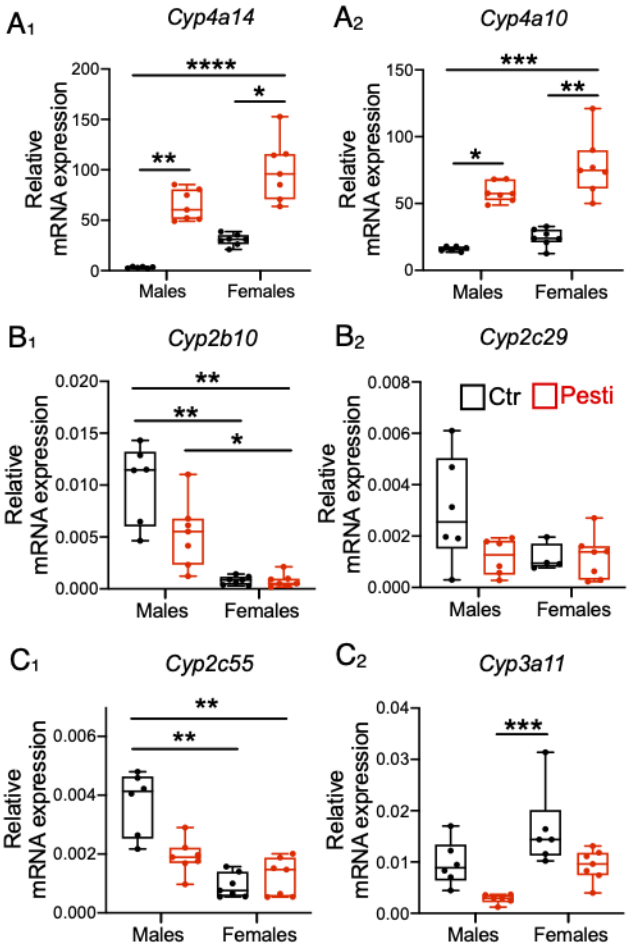
A1
Cyp4a14
Relative mRNA expression
200
150
100
50
0
****
*
**
Males
Females
A2
Cyp4a10
Relative mRNA expression
150
100
50
0
***
**
*
Males
Females
B1
Cyp2b10
Relative mRNA expression
0.020
0.015
0.010
0.005
0.000
**
**
*
Males
Females
B2
Cyp2c29
Ctr
Pesti
Relative mRNA expression
0.008
0.006
0.004
0.002
0.000
Males
Females
C1
Cyp2c55
Relative mRNA expression
0.006
0.004
0.002
0.000
**
**
Males
Females
C2
Cyp3a11
Relative mRNA expression
0.04
0.03
0.02
0.01
0.00
***
Males
Females

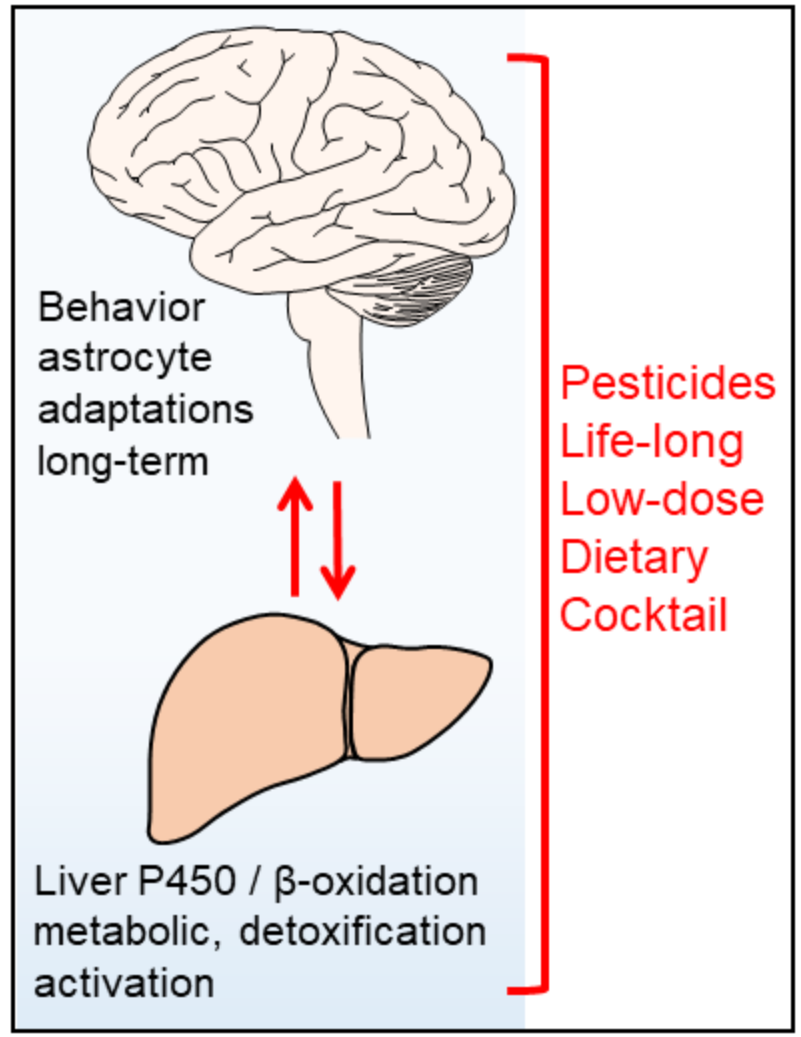
Behavior
astrocyte
adaptations
long-term
Liver P450 / β-oxidation
metabolic, detoxification
activation
Pesticides
Life-long
Low-dose
Dietary
Cocktail